

Research Article

Targeted Photodynamic Virotherapy Armed with a Genetically Encoded Photosensitizer

Kiyoto Takehara¹, Hiroshi Tazawa^{1,2}, Naohiro Okada¹, Yuuri Hashimoto¹,
Satoru Kikuchi¹, Shinji Kuroda¹, Hiroyuki Kishimoto¹, Yasuhiro Shirakawa¹,
Nobuhiro Narii³, Hiroyuki Mizuguchi³, Yasuo Urata⁵,
Shunsuke Kagawa¹, and Toshiyoshi Fujiwara¹

Author's Affiliations

¹Department of Gastroenterological Surgery, Okayama University Graduate School of Medicine, Dentistry and Pharmaceutical Sciences, Okayama 700-8558, Japan; ²Center for Innovative Clinical Medicine, Okayama University Hospital, Okayama 700-8558, Japan; ³Laboratory of Biochemistry and Molecular Biology, Graduate School of Pharmaceutical Sciences, Osaka University, Osaka 565-0871, Japan; ⁴Oncolys BioPharma, Inc., Tokyo, 106-0032, Japan.

Corresponding Author: Toshiyoshi Fujiwara, Department of Gastroenterological Surgery, Okayama University Graduate School of Medicine, Dentistry, and Pharmaceutical Sciences, 2-5-1 Shikata-cho, Kita-ku, Okayama 700-8558, Japan. Phone: 81-86-235-7255; Fax: 81-86-221-8775; E-mail: toshi_f@md.okayama-u.ac.jp.

Footnotes:

Abbreviations: PDT, photodynamic therapy; ROS, reactive oxygen species; GFP, green fluorescent protein; Ad, non-replicative adenovirus; hTERT, human telomerase reverse transcriptase; IRES, internal ribosome entry site; DCF-DA, 2',7'-Dichlorodihydrofluorescein Diacetate; PBS, phosphate buffered saline; MOI, multiplicity of infection; PFU, plaque-forming unit; XTT, sodium 3'-[1-(phenylaminocarbonyl)-3,4-tetrazolium]-bis(4-methoxy-6-nitro)benzene sulfonic acid hydrate.

Running title: KillerRed-based oncolytic photodynamic therapy.

Key words: Photodynamic therapy; KillerRed; adenovirus; telomerase; ROS.

Disclosure of Potential Conflicts of Interest: Y. Urata is President & CEO of Oncolys BioPharma, Inc., the manufacturer of OBP-301 (Telomelysin). H. Tazawa and T. Fujiwara are consultants of Oncolys BioPharma, Inc. No potential conflicts of interest were disclosed by the other authors.

Grant Support: This study was supported by grants from the Ministry of Health, Labour, and Welfare of Japan (to T. Fujiwara; No. 10103827, No. 13801426, No. 14525167) and by grants from the Ministry of Education, Culture, Sports, Science and Technology, Japan (T. Fujiwara; No. 25293283).

Abstracts

Photodynamic therapy (PDT) is a minimally invasive antitumor therapy that eradicates tumor cells through a photosensitizer-mediated cytotoxic effect upon light irradiation. However, systemic administration of photosensitizer often makes it difficult to avoid a photosensitive adverse effect. A red fluorescent protein KillerRed generates reactive oxygen species (ROS) upon green light irradiation. Here we show the therapeutic potential of a novel tumor-specific replicating photodynamic viral agent (TelomeKiller) constructed by using the human telomerase reverse transcriptase (hTERT) promoter. We investigated the light-induced antitumor effect of TelomeKiller in several types of human cancer cell lines. Relative cell viability was investigated using an XTT assay. The *in vivo* antitumor effect was assessed using subcutaneous xenografted tumor and lymph node metastasis models. KillerRed accumulation resulted in ROS generation and apoptosis in light-irradiated cancer cells. Intratumoral injection of TelomeKiller efficiently delivered the KillerRed protein throughout the tumors and exhibited a long-lasting antitumor effect with repeated administration and light irradiation in mice. Moreover, intratumorally injected TelomeKiller could spread into the regional lymph node area and eliminate micrometastasis with limited-field laser irradiation. Our results suggest that KillerRed has great potential as a novel photosensitizer if delivered with a tumor-specific virus-mediated delivery system. TelomeKiller-based PDT is a promising antitumor strategy to efficiently eradicate tumor cells.

Introduction

Photodynamic therapy (PDT) is a minimally invasive antitumor strategy for the induction of tumor-specific cytotoxicity through the accumulation of photosensitizers and subsequent light irradiation (1, 2). Light irradiation of a specific wavelength induces the photosensitizer-mediated generation of reactive oxygen species (ROS) and subsequent cytotoxicity in tumor cells. Currently, photosensitizers such as Photofrin, Talaporfin (Laserphyrin) and 5-aminolevulinic acid are frequently used for anticancer PDT in a clinical setting (2). Although Photofrin is the most popular photosensitizer used worldwide, there are a number of unsolved problems with the use of photosensitizers, including a long-lasting skin photosensitivity and low efficacy of elimination of tumor cells. The lack of sufficient and continuous accumulation of photosensitizers in tumor tissues often makes it difficult to eradicate tumor cells by PDT. Therefore, the development of a novel strategy for more efficient and persistent tumor-specific accumulation of photosensitizers in tumor tissues is required to improve the antitumor effect of PDT.

KillerRed is a novel bioengineered dimeric red fluorescent protein that was obtained from genetically engineered green fluorescent protein (GFP) homologs (3). KillerRed generates ROS upon green light irradiation with fluorescence excitation/emission maxima at 585/610 nm (3), suggesting a therapeutic potential of KillerRed as a novel photosensitizer. In fact, recent reports have shown that KillerRed, but not other red fluorescent proteins, can induce a phototoxic effect in a light-mediated manner in *Escherichia coli* bacteria (3, 4) and in normal human kidney 293T cells (3, 5). Moreover, some recent reports have suggested the therapeutic potential of KillerRed as a novel photosensitizer against tumor cells (6, 7). If KillerRed protein was efficiently and persistently accumulated in tumor cells, then green light

irradiation would induce a KillerRed-mediated cytotoxic effect. However, a delivery system for tumor-specific KillerRed accumulation is required to develop KillerRed-based photodynamic anticancer therapy.

Genetically engineered armed oncolytic viruses that express several types of therapeutic transgenes have recently been reported that were aimed at enhancing the antitumor effect of an oncolytic virus (8, 9). A telomerase-specific replicative oncolytic adenovirus (OBP-301, Telomelysin), in which the human telomerase reverse transcriptase (hTERT) promoter element drives *E1* gene expression, selectively replicates in tumor cells and lyses infected cells (10-12). In addition to its inherent cytotoxicity, Telomelysin can also be used as vectors for gene delivery (13-16). We further modified Telomelysin to contain the *KillerRed* gene for targeted photodynamic virotherapy. Here we show the therapeutic potential of a telomerase-specific conditionally replicating adenovirus expressing KillerRed, termed TelomeKiller, by using a subcutaneous xenografted tumor model and an intraperitoneal lymph node metastasis model.

Materials and Methods

Cell lines

The human non-small cell lung cancer cell line H1299 and the human colon cancer cell lines HCT116 and HT-29 were obtained from the American Type Culture Collection (Manassas, VA, USA). HCT-116-GFP cells that express GFP protein were obtained from AntiCancer Inc. (SanDiego, CA, USA). H1299 and HCT116-GFP cells were maintained in RPMI-1640 medium. HCT116 and HT-29 cells were maintained in McCoy's 5A and Dulbecco's modified Eagle's medium, respectively. All media were supplemented with 10%

fetal bovine serum, 100 U/ml penicillin and 100 mg/ml streptomycin. The cells were routinely maintained at 37 °C in a humidified atmosphere with 5% CO₂ and not cultured for more than 5 months following resuscitation. The authentication was not performed by the authors. H1299 cells stably transfected with pKillerRed-mem (H1299-KillerRed) or pTurboFP635 (H1299-TurboFP635) or co-transfected with pKillerRed-mem and pEGFP (H1299-KillerRed-EGFP) were established by a limiting dilution method.

Recombinant adenoviruses

The recombinant non-replicative E1/E3-deleted adenovirus expressing cytotoxic KillerRed (Ad-KillerRed) or non-cytotoxic TurboFP635 (Ad-TurboFP635) was generated by insertion into the virus of the KillerRed or the TurboFP635 gene expression cassette, respectively, which was excised from the membrane-targeted KillerRed expression plasmid pKillerRed-mem (Evrogen, Moscow, Russia) or the TurboFP635 expression plasmid (Evrogen) (Supplementary Fig. S1A). The telomerase-specific conditionally replicating adenovirus OBP-301 (Telomelysin), in which the promoter element of the human telomerase reverse transcriptase (*hTERT*) gene drives the expression of *E1A* and *E1B* genes that are linked with an internal ribosome entry site (IRES), was previously constructed and characterized (10, 11) (Supplementary Fig. S1B). For tumor-specific induction of KillerRed expression by OBP-301, the KillerRed-expressing conditionally replicating replication-competent adenovirus (TelomeKiller) was generated, in which a KillerRed expression cassette was inserted into the *E3* region of OBP-301 (Supplementary Fig. S1B). Recombinant adenoviruses were purified using cesium chloride step gradients, their titers were determined by a plaque-forming assay using 293 cells, and they were stored at -80 °C.

Detection of intracellular reactive oxygen species

To detect the generation of intracellular reactive oxygen species (ROS), 2',7'-Dichlorodihydrofluorescein Diacetate (DCF-DA) (Wako) was used. H1299 and H1299-KillerRed cells were incubated with DCF-DA (20 μ M) for 30 min at 37 °C, and after washing twice with phosphate buffered saline (PBS), fluorescence was detected at 485/528 nm using a fluorescence microplate reader.

Immunocytochemistry for cleaved caspase-3

H1299-KillerRed cells were irradiated with green light (200 mW/cm²) through semrock fluorescence filter (542-582 nm) (TxRed-4040C-000) for 60 min (720 kJ/cm²) using a fluorescence microscope (IX71; Olympus, Tokyo, Japan). The irradiance was measured using power meter, PM100D (Thorlabs, Inc., Tokyo, Japan). Twenty-four hours after irradiation, the H1299-KillerRed cells were fixed with 3% paraformaldehyde solution for 15 min and permeabilized with 0.2% Triton X-100 in Blocking-One solution (Nacalai Tesque, Kyoto, Japan) for 5 min. After washing with PBS, cells were incubated with rabbit anti-cleaved caspase-3 monoclonal antibody (Cell Signaling Technology) and FITC-conjugated secondary antibody. After nuclear staining with DAPI, the cells were observed using a fluorescent microscope (IX71; Olympus).

Cell viability assay

Cells were seeded on 96-well plates at a density of 3×10^3 cells/well 24 hours before infection and were infected with Ad-KillerRed or Ad-TurboFP635 at multiplicity of infections (MOIs) of 0, 10, 50, 100, 500 or 1000 plaque-forming units (PFU)/cell or with TelomeKiller at MOIs of 0, 10, 50 or 100 PFU/cell. Cells were irradiated with 590 nm

yellow-orange LED light (180 mW/cm²) for 60 min (648 kJ/cm²) on the first two days following virus infection. Cell viability was determined immediately after irradiation using the Cell Proliferation Kit II (Roche Molecular Biochemicals, Indianapolis, IN, USA) which is based on an XTT, (sodium 3'-[1-(phenylaminocarbonyl)-3,4-tetrazolium]-bis(4-methoxy-6-nitro) benzene sulfonic acid hydrate) assay, according to the manufacturer's protocol. Cell viability of Ad-KillerRed- or Ad-TurboFP635-infected cells was calculated by dividing the viability of irradiated cells by that of non-irradiated cells, and the viability of TelomeKiller-infected cells was calculated as the percentage of viable infected cells divided by that of viable non-infected cells.

Western blot analysis

H1299 or H1299-KillerRed cells were seeded on 6-well plates at a density of 5×10^4 cells/well. H1299 cells were further infected with Ad-KillerRed or TelomeKiller at an MOI of 100. Whole cell lysates were prepared in a lysis buffer (50 mM Tris-HCl (pH 7.4), 150 mM NaCl, 1% Triton X-100) containing a protease inhibitor cocktail (Complete Mini; Roche Applied Science, Mannheim, Germany). Proteins were electrophoresed on 10% SDS polyacrylamide gels and were transferred to polyvinylidene difluoride membranes (Hybond-P; GE Health Care, Buckinghamshire, UK). Blots were blocked with 5% non-fat dry milk in Tris-buffered saline and 0.1% Tween-20, pH 7.4 (TBS-T) at room temperature for 30 min. The primary antibodies used were: rabbit anti-KillerRed polyclonal antibody (Evrogen), and mouse anti- β -actin monoclonal antibody (Sigma-Aldrich, St. Louis, MO, USA). The secondary antibodies used were: horseradish peroxidase-conjugated antibodies against rabbit IgG (GE Healthcare), or mouse IgG (GE Healthcare). Immunoreactive bands

on the blots were visualized using enhanced chemiluminescence substrates (ECL Prime; GE Healthcare).

***In vivo* subcutaneous HCT116 tumor model**

The experimental protocol was approved by the Ethics Review Committee for Animal Experimentation of our institution. HCT116-GFP xenograft tumors were produced on the left flank of 6-week-old female BALB/C-*nu/nu* mice by subcutaneous injection of 3×10^6 cells in 50 μ l of PBS with 50 μ l of Matrigel basement membrane matrix (BD biosciences, Bedford, MA, USA). As the tumors grew to a diameter of 6 to 7 mm, TelomeKiller was injected intra-tumorally at an MOI of 1.0×10^8 PFU/100 μ l. Mice were anesthetized by subcutaneous injection of ketamine (100 mg/kg) and xylazine (10 mg/kg). PDT was performed using a 589 nm Diode Pumped Solid State Laser (Changchun New Industries Optoelectronics Technology Co., Ltd., Changchun, P.R. China). The mice were irradiated with yellow-orange laser (300 mW/cm²) for 30 min (1.08 MJ/cm²). Virus was injected on days 0, 7 and 14 and laser irradiation was performed on days 3 and 4, 10 and 11, and 17 and 18. The perpendicular diameter of each tumor was measured every 3 or 4 days, and tumor volume was calculated using the following formula: tumor volume (mm³) = $a \times b^2 \times 0.5$, where a is the longest diameter, b is the shortest diameter, and 0.5 is a constant for calculation of the volume of an ellipsoid. The tumors were excised on day 28.

***In vivo* HCT116-GFP lymph node metastasis model**

The implantation procedures for submucosally invasive early human rectal cancer xenograft tumors have recently been established (17). Briefly, cell suspensions of HCT116-GFP cells at a density of 3×10^6 cells in 25 μ l of PBS with 25 μ l of Matrigel

basement membrane matrix were slowly injected into the submucosal layer of the rectum using a 29-gauge needle. Ten days later, as the rectal tumors grew to a diameter of about 5 mm, 1.0×10^8 PFU/50 μ l of TelomeKiller were directly injected into the rectal tumors. Three days after virus injection, laparotomy was performed and GFP-expressing metastatic para-aortic or iliac lymph nodes were irradiated with the laser at 300 mW/cm^2 for 30 min (1.08 MJ/cm^2). Twenty-one days after virus injection, the mice were euthanized to assess tumor progression in the lymph nodes. *In vivo* fluorescence images were taken using a stereo microscope (SZX16; Olympus) and a microscope digital camera (DP71; Olympus). GFP fluorescence intensity was analyzed using VisionWorks LS software for the quantification of lymph node metastasis.

Statistical analysis

Data are expressed as means \pm SD. Significant differences were assessed using Student's *t*-test. Statistical significance was defined when the *P* value was less than 0.05.

Results

KillerRed-mediated apoptosis induction in human cancer cells via increased intracellular reactive oxygen species

To investigate whether KillerRed induces ROS and apoptosis in human cancer cells, human lung cancer H1299 cells that were stably transfected with a cytotoxic KillerRed-expression plasmid vector (H1299-KillerRed) or a non-cytotoxic TurboFP635 expression plasmid vector (H1299-TurboFP635) were established. When parental H1299, H1299-KillerRed and H1299-TurboFP635 cells were irradiated with green light for 60 min, a

dramatic morphological change to a rounded shape was observed in H1299-KillerRed cells, but not in H1299 or H1299-TurboFP635 cells (Fig. 1A). We further confirmed that H1299 cells stably co-transfected with KillerRed- and EGFP-expressing vectors (H1299-KillerRed-EGFP) showed morphological changes following photobleaching during light irradiation (Supplementary Movie S1). Analysis of intracellular ROS using DCF-DA revealed that the intracellular amount of ROS was significantly increased in H1299-KillerRed cells after light irradiation compared to the parental H1299 cells (Fig. 1B). Moreover, immunocytological analysis demonstrated that expression of the apoptosis-specific marker cleaved caspase-3 was increased in the light-irradiated H1299-KillerRed cells (Fig. 1C). These results suggest that KillerRed accumulation induces apoptotic cell death in association with oxidative stress in human cancer cells.

Photosensitive antitumor effect of KillerRed induced by a non-replicative adenovirus

The observation of KillerRed-mediated apoptosis induction in light-irradiated cancer cells prompted us to develop a virus-mediated KillerRed delivery system as a novel photodynamic anticancer therapy. Since replication-deficient adenovirus vectors are frequently used to induce therapeutic genes such as tumor suppressor p53 (18) in human cancer cells in preclinical and clinical settings, we generated a replication-deficient adenovirus vector expressing cytotoxic KillerRed (Ad-KillerRed) or non-cytotoxic TurboFP635 (Ad-TurboFP635) (Supplementary Fig. S1A). Three types of human cancer cell lines (H1299, HCT116, HT-29) were infected with Ad-KillerRed or Ad-TurboFP635 at an MOI of 100. After infection for 48 hours, the virus-infected cells were irradiated with green light for 60 min (Fig. 2). The Ad-KillerRed-infected cancer cells showed photobleaching and morphological change to a rounded shape and shrinkage after light irradiation. In contrast,

Ad-TurboFP635-infected cancer cells showed no photobleaching and slight morphological change to a rounded shape after light irradiation. To quantitatively compare the antitumor effect of Ad-KillerRed and Ad-TurboFP635, the viability of virus-infected human cancer cells with or without light irradiation was analyzed using an XTT assay. Infection with Ad-KillerRed at an MOI of 100 significantly decreased the viability of H1299 cells following photobleaching at 60 min after infection (Fig. 3A). Ad-KillerRed infection at high doses (MOIs of 100, 500, and 1000) significantly decreased the viability of H1299 and HCT116 cells after light irradiation, whereas Ad-KillerRed at MOI of more than 500 was needed to reduce the viability of HT-29 cells after light irradiation (Fig. 3B). In contrast, Ad-TurboFP635 infection did not affect the viability of human cancer cells after light irradiation (Fig. 3C). These results suggest that the adenovirus-mediated KillerRed delivery system is a useful method for induction of the KillerRed-mediated antitumor effect in human cancer cells in combination with light irradiation.

Profound antitumor effect of KillerRed induced by a conditionally replicating adenovirus

To induce KillerRed expression in human cancer cells in a more efficient and tumor-specific manner than could be achieved with Ad-KillerRed, we further generated a telomerase-specific conditionally replicating adenovirus that expressed KillerRed (TelomeKiller) (Supplementary Fig. S1B). When the expression level of KillerRed in Ad-KillerRed- and TelomeKiller-infected H1299 cells was compared using western blot analysis, TelomeKiller cells induced higher KillerRed expression than Ad-KillerRed cells in a time-dependent manner (Fig. 4A). The KillerRed expression induced by the Ad-KillerRed cells was similar to that of the H1299-KillerRed stable transfectants. Under fluorescence

microscopy, TelomeKiller efficiently induced red fluorescent KillerRed expression and morphological change to a rounded shape in 3 different human cancer cell lines before light irradiation because TelomeKiller has cytopathic effect due to virus replication (Fig. 4B). After light irradiation, TelomeKiller-infected cancer cells showed photobleaching and morphological change to shrinkage and destruction of cell membrane (Fig. 4B). Moreover, an XTT assay demonstrated that light irradiation significantly enhanced the TelomeKiller-mediated antitumor effect in HCT116 and HT-29 cells, whereas H1299 cells were highly sensitive to TelomeKiller infection alone (Fig. 4C). These results suggest that TelomeKiller-based KillerRed delivery system is a useful method for the induction of high KillerRed accumulation and for KillerRed-mediated antitumor effect in combination with light irradiation.

***In vivo* antitumor effect of TelomeKiller in an HCT116 xenograft tumor model in combination with light irradiation**

Next, to evaluate the TelomeKiller-mediated *in vivo* antitumor effect, we first investigated the tumor distribution of KillerRed expression using subcutaneous HCT116 xenograft tumor models. TelomeKiller was injected at a concentration of 1.0×10^8 PFU/100 μ l into the left tumor and 100 μ l of PBS was injected into the right tumor. Four days after virus injection, fluorescence images were acquired under a fluorescence stereomicroscope. Slight KillerRed-mediated red fluorescence was observed throughout the body surface of the mice with TelomeKiller-injected tumor tissues (Fig. 5A). Analysis of isolated tumors indicated that red fluorescence was widely distributed within TelomeKiller-injected tumor tissues (Fig. 5B).

Based on the result of the KillerRed distribution experiment, we next assessed the *in vivo* antitumor effect of TelomeKiller in combination with light irradiation using this human HCT116 xenograft tumor model. HCT116 tumors were treated with 1) nothing (control), 2) TelomeKiller injection alone, 3) light irradiation alone, or 4) combination therapy of TelomeKiller injection and light irradiation (Fig. 5C). Combination therapy of TelomeKiller and light irradiation significantly suppressed tumor growth when compared with control or TelomeKiller injection alone. Analysis of the tumor macroscopic appearance showed that combination therapy-treated tumors were small with surface scar tissues (Fig. 5D). Upon histopathological analysis, large necrotic areas were observed in combination therapy-treated tumors, but not in control, TelomeKiller- or light irradiation-treated tumors (Fig. 5E). These results suggested that combination therapy of TelomeKiller and light irradiation efficiently eliminated tumor cells.

***In vivo* ablation of lymph node metastasis by the combination of TelomeKiller infection and light irradiation**

Finally, we investigated whether intratumoral injection of TelomeKiller in combination with laser irradiation could ablate regional lymph node metastasis in a colorectal cancer HCT116-GFP xenograft tumor model. We recently established an orthotopic early rectal cancer xenograft model with spontaneous lymph node metastasis by implantation of GFP-labeled HCT116-GFP cells (17). Using this animal model, TelomeKiller was injected directly into the rectal HCT116-GFP tumors, which grew to a diameter of about 5 mm with GFP-labeled lymph node metastasis (Fig. 6A). Three days after virus injection, KillerRed and GFP-expressing metastatic lymph nodes were irradiated with a yellow-orange laser (Fig. 6B). Twenty-one days after virus injection, GFP-positive metastatic lymph nodes decreased in size

in 4 out of 4 mice that received both the TelomeKiller injection and laser irradiation. In contrast, GFP-positive metastatic lymph nodes increased in size in 5 out of 6 mice that received TelomeKiller injection without laser irradiation. The non-treated control group demonstrated enlargement of GFP-positive metastatic lymph nodes in 3 out of 3 mice (Figs. 6C and 6D). The GFP fluorescence intensity of metastatic lymph nodes was decreased in TelomeKiller + PDT group compared to control and TelomeKiller groups, although there was no significant difference (Supplementary Fig. S2). These results suggested that TelomeKiller in combination with light irradiation induced an antitumor effect against regional lymph node metastasis.

Discussion

PDT is a promising minimally invasive anticancer therapy that induces photosensitizer-mediated cell death in combination with light irradiation. Although some kinds of conventional photosensitizers have been systemically administered for PDT in clinical settings (2), the therapeutic potential of PDT is often reduced by the lack of a tumor-specific delivery system for the photosensitizer. In this study, we developed a tumor-specific virus-mediated delivery system for the photosensitive cytotoxic KillerRed, by using a telomerase-specific conditionally replicating TelomeKiller. Tumor-specific replicative TelomeKiller induced much higher KillerRed expression compared with replication-defective Ad-KillerRed. TelomeKiller efficiently induced *in vitro* and *in vivo* antitumor effects in combination with light irradiation. Moreover, the formation of metastatic lymph nodes was also suppressed in TelomeKiller-treated tumors when combined with light irradiation. Thus, this tumor-specific replicating virus-mediated KillerRed delivery system is a promising PDT

strategy for suppression of the growth of primary tumors and regional lymph node metastasis through a KillerRed-mediated phototoxic effect.

A tumor-specific replicating adenovirus-mediated KillerRed delivery system has some advantages compared to conventional photosensitizer. The first advantage is the high tumor selectivity of KillerRed accumulation, which is achieved by using a telomerase-specific replicating adenovirus. Although systemic administration of conventional photosensitizer often causes light-induced adverse effects because of photosensitizer accumulation in normal tissues, TelomeKiller would reduce the risk of a photosensitivity disorder owing to the tumor-specific KillerRed accumulation. The second advantage is the high and prolonged KillerRed accumulation that can be achieved by using a replication-competent adenovirus. TelomeKiller increases KillerRed expression in a time-dependent manner by virus replication. In contrast, the accumulation of conventional photosensitizer in tumor cells would decrease in a time-dependent manner after administration. The third advantage is the profound dual antitumor effects mediated by KillerRed-mediated cell death and virus-mediated cell lysis. TelomeKiller suppressed the viability of non-irradiated human cancer cells and light irradiation significantly enhanced the antitumor effect of TelomeKiller. In contrast, the therapeutic potential of conventional photosensitizer-based PDT depends mainly on the photosensitizer-mediated cytotoxic effect upon light irradiation (2). Taking these possible advantages into consideration, a TelomeKiller-based PDT strategy would induce a more profound antitumor effect compared to conventional PDT through KillerRed-mediated phototoxicity and virus-mediated oncolysis.

Regarding the mechanism underlying the KillerRed-induced cytotoxic effect, we observed the involvement of intracellular ROS generation and apoptosis induction. Previous reports have suggested that light-mediated KillerRed activation induces ROS generation (3,

5) and apoptosis (5, 7) and these data are consistent with our results. Analysis of KillerRed structure by an X-ray (19) and a high-resolution crystallographic study (20) revealed that a water-filled channel that reacts with the chromophore is responsible for the generation of ROS, which is mainly comprised of singlet oxygen (3, 21). The intracellular localization of KillerRed that generates ROS is an especially critical factor for KillerRed-mediated cell cytotoxicity. Williams *et al.* (22) recently showed that KillerRed expression in mitochondria induces only organelle fragmentation, but that its expression in the plasma membrane induces cell death upon light irradiation of the neurons of *C. elegans*. Consistent with these data, a cell membrane-bound KillerRed expression induces apoptotic cell death upon light irradiation in zebrafish (23) and *Xenopus laevis* (24). In the present study, we used a cell membrane-targeted KillerRed expression vector for the plasmid-based transfection assay and for the development of the Ad-KillerRed and TelomeKiller viruses. Thus, the destruction of cell membrane by KillerRed-induced ROS generation may be the mechanism by which it induces apoptosis in human cancer cells.

Conventional photosensitizer-mediated PDT is limited to early stage tumors without metastatic regions in clinical settings (2). However, in combination with light irradiation TelomeKiller significantly suppressed the growth of not only the subcutaneous xenograft tumor but also of lymph node metastasis. These findings suggest that TelomeKiller-based PDT is a promising antitumor strategy for advanced cancer patients with metastatic tumors. We previously reported that intratumoral injection of a telomerase-specific replication-competent adenovirus Telomelysin suppressed the growth of a subcutaneous xenograft tumor (10) and of lymph node metastasis of an orthotopic colorectal cancer model (17, 25). Moreover, an GFP-expressing Telomelysin (OBP-301, TelomeScan) could induce tumor-specific GFP accumulation in the metastatic regions at lymph nodes (13, 26), liver (27),

and peritoneal cavities (28) of colorectal tumor-bearing mice. These findings strongly suggest that a TelomeKiller-based PDT strategy is a useful anticancer strategy to eliminate metastatic tumors.

There are some issues that remain to be resolved for clinical application of TelomeKiller in PDT. The first issue is the presence of adenovirus-neutralizing antibody. Clinical studies of the tumor suppressor p53-expressing replication-deficient adenovirus, Ad-p53, have already shown that administration of Ad-p53 by intratumoral, intraperitoneal or intravesical injection is a safe and feasible antitumor therapy (18), whereas the therapeutic potential of its systemic intravenous administration is less than ideal, because an injected adenovirus vector is attenuated by neutralizing antibody in the blood circulation. Recently, it has been reported that a pH-responsive charge reversal polymeric complex could be successfully used to deliver plasmid DNA of KillerRed to tumors in athymic nude mice following systemic administration (29); however, as PDT itself is a local therapy because the irradiation field is limited, the regional spread of intratumorally injected TelomeKiller might be sufficient to induce the therapeutic benefit. The second issue is the development of light irradiation devices for optimal KillerRed activation. Although yellow-orange light with an excitation wavelength of 585 nm is required to activate KillerRed, yellow-orange light cannot reach deeper than 2 mm in tissues (2). Therefore, the therapeutic target of a TelomeKiller-based PDT strategy would be limited to primary tumors and to metastatic regions at superficial areas where light irradiation can reach. In contrast, long time and frequent exposure of light irradiation was done to obtain the therapeutic potential of TelomeKiller-based PDT in *in vitro* and *in vivo* experiments. As light irradiation alone slightly reduced the tumor volume compared to control group (Fig. 5C), high light irradiation may induce considerable heat generation and the antitumor effect as hyperthermia, probably

contributing to the discrepancy of antitumor effect between *in vitro* and *in vivo* experiments. Moreover, as high light irradiation-induced photobleaching may attenuate the ROS generation, lower light irradiation may produce more antitumor effect of KillerRed with less photobleaching and more ROS generation. To overcome these limitations, further experiments aimed at developing the more appropriate light irradiation devices are warranted for clinical application of the TelomeKiller-based PDT strategy.

In conclusion, we clearly demonstrated that a telomerase-specific conditionally replicating KillerRed-expressing adenovirus, TelomeKiller, efficiently inhibits cell viability, tumor growth and lymph node metastasis in human cancer cells through a KillerRed-mediated photosensitive cytotoxic effect. A phase I clinical trial of Telomelysin in patients with advanced solid tumors has recently been completed and Telomelysin was well tolerated by these patients (30). Although the cytotoxicity of TelomeKiller in cancer patients remains to be elucidated, a conditionally replicating adenovirus-mediated KillerRed delivery system would provide a novel anticancer strategy to improve the therapeutic potential of PDT.

Acknowledgements

We thank Ms. Tomoko Sueishi for her technical support.

References

1. Castano AP, Mroz P, Hamblin MR. Photodynamic therapy and anti-tumour immunity. *Nat Rev Cancer*. 2006;6:535-45.
2. Agostinis P, Berg K, Cengel KA, Foster TH, Girotti AW, Gollnick SO, et al. Photodynamic therapy of cancer: an update. *CA: a cancer journal for clinicians*. 2011;61:250-81.
3. Bulina ME, Chudakov DM, Britanova OV, Yanushevich YG, Staroverov DB, Chepurnykh TV, et al. A genetically encoded photosensitizer. *Nat Biotechnol*. 2006;24:95-9.
4. Waldeck W, Heidenreich E, Mueller G, Wiessler M, Toth K, Braun K. ROS-mediated killing efficiency with visible light of bacteria carrying different red fluorochrome proteins. *Journal of photochemistry and photobiology B, Biology*. 2012;109:28-33.
5. Liao ZX, Li YC, Lu HM, Sung HW. A genetically-encoded KillerRed protein as an intrinsically generated photosensitizer for photodynamic therapy. *Biomaterials*. 2014;35:500-8.
6. Serebrovskaya EO, Edelweiss EF, Stremovskiy OA, Lukyanov KA, Chudakov DM, Deyev SM. Targeting cancer cells by using an antireceptor antibody-photosensitizer fusion protein. *Proc Natl Acad Sci U S A*. 2009;106:9221-5.
7. Shirmanova MV, Serebrovskaya EO, Lukyanov KA, Snopova LB, Sirotkina MA, Prodanetz NN, et al. Phototoxic effects of fluorescent protein KillerRed on tumor cells in mice. *Journal of biophotonics*. 2013;6:283-90.
8. Liu TC, Galanis E, Kirn D. Clinical trial results with oncolytic virotherapy: a century of promise, a decade of progress. *NatClinPractOncol*. 2007;4:101-17.
9. Cody JJ, Douglas JT. Armed replicating adenoviruses for cancer virotherapy. *Cancer Gene Ther*. 2009;16:473-88.
10. Kawashima T, Kagawa S, Kobayashi N, Shirakiya Y, Umeoka T, Teraishi F, et al. Telomerase-specific replication-selective virotherapy for human cancer. *ClinCancer Res*. 2004;10:285-92.
11. Hashimoto Y, Watanabe Y, Shirakiya Y, Uno F, Kagawa S, Kawamura H, et al. Establishment of biological and pharmacokinetic assays of telomerase-specific replication-selective adenovirus. *Cancer Sci*. 2008;99:385-90.

12. Sasaki T, Tazawa H, Hasei J, Kunisada T, Yoshida A, Hashimoto Y, et al. Preclinical evaluation of telomerase-specific oncolytic virotherapy for human bone and soft tissue sarcomas. *Clin Cancer Res.* 2011;17:1828-38.
13. Kishimoto H, Kojima T, Watanabe Y, Kagawa S, Fujiwara T, Uno F, et al. In vivo imaging of lymph node metastasis with telomerase-specific replication-selective adenovirus. *Nat Med.* 2006;12:1213-9.
14. Kojima T, Hashimoto Y, Watanabe Y, Kagawa S, Uno F, Kuroda S, et al. A simple biological imaging system for detecting viable human circulating tumor cells. *J Clin Invest.* 2009;119:3172-81.
15. Yamasaki Y, Tazawa H, Hashimoto Y, Kojima T, Kuroda S, Yano S, et al. A novel apoptotic mechanism of genetically engineered adenovirus-mediated tumour-specific p53 overexpression through E1A-dependent p21 and MDM2 suppression. *Eur J Cancer.* 2012;48:2282-91.
16. Shigeyasu K, Tazawa H, Hashimoto Y, Mori Y, Nishizaki M, Kishimoto H, et al. Fluorescence virus-guided capturing system of human colorectal circulating tumour cells for non-invasive companion diagnostics. *Gut.* 2015;64:627-35.
17. Kikuchi S, Kishimoto H, Tazawa H, Hashimoto Y, Kuroda S, Nishizaki M, et al. Biological ablation of sentinel lymph node metastasis in submucosally invaded early gastrointestinal cancer. *Mol Ther.* 2015;23:501-9.
18. Tazawa H, Kagawa S, Fujiwara T. Advances in adenovirus-mediated p53 cancer gene therapy. *Expert Opin Biol Ther.* 2013;13:1569-83.
19. Carpentier P, Violot S, Blanchoin L, Bourgeois D. Structural basis for the phototoxicity of the fluorescent protein KillerRed. *FEBS Lett.* 2009;583:2839-42.
20. Pletnev S, Gurskaya NG, Pletneva NV, Lukyanov KA, Chudakov DM, Martynov VI, et al. Structural basis for phototoxicity of the genetically encoded photosensitizer KillerRed. *J Biol Chem.* 2009;284:32028-39.
21. Roy A, Carpentier P, Bourgeois D, Field M. Diffusion pathways of oxygen species in the phototoxic fluorescent protein KillerRed. *Photochemical & photobiological sciences : Official journal of the European Photochemistry Association and the European Society for Photobiology.* 2010;9:1342-50.

22. Williams DC, Bejjani RE, Ramirez PM, Coakley S, Kim SA, Lee H, et al. Rapid and permanent neuronal inactivation in vivo via subcellular generation of reactive oxygen with the use of KillerRed. *Cell reports*. 2013;5:553-63.
23. Teh C, Chudakov DM, Poon KL, Mamedov IZ, Sek JY, Shidlovsky K, et al. Optogenetic in vivo cell manipulation in KillerRed-expressing zebrafish transgenics. *BMC Dev Biol*. 2010;10:110.
24. Jewhurst K, Levin M, McLaughlin KA. Optogenetic Control of Apoptosis in Targeted Tissues of *Xenopus laevis* Embryos. *Journal of cell death*. 2014;7:25-31.
25. Kojima T, Watanabe Y, Hashimoto Y, Kuroda S, Yamasaki Y, Yano S, et al. In vivo biological purging for lymph node metastasis of human colorectal cancer by telomerase-specific oncolytic virotherapy. *AnnSurg*. 2010;251:1079-86.
26. Kurihara Y, Watanabe Y, Onimatsu H, Kojima T, Shirota T, Hatori M, et al. Telomerase-specific virotheranostics for human head and neck cancer. *Clin Cancer Res*. 2009;15:2335-43.
27. Kishimoto H, Urata Y, Tanaka N, Fujiwara T, Hoffman RM. Selective metastatic tumor labeling with green fluorescent protein and killing by systemic administration of telomerase-dependent adenoviruses. *Mol Cancer Ther*. 2009;8:3001-8.
28. Kishimoto H, Zhao M, Hayashi K, Urata Y, Tanaka N, Fujiwara T, et al. In vivo internal tumor illumination by telomerase-dependent adenoviral GFP for precise surgical navigation. *Proc Natl Acad Sci U S A*. 2009;106:14514-7.
29. Tseng SJ, Liao ZX, Kao SH, Zeng YF, Huang KY, Li HJ, et al. Highly specific in vivo gene delivery for p53-mediated apoptosis and genetic photodynamic therapies of tumour. *Nat Commun*. 2015;6:6456.
30. Nemunaitis J, Tong AW, Nemunaitis M, Senzer N, Phadke AP, Bedell C, et al. A phase I study of telomerase-specific replication competent oncolytic adenovirus (telomelysin) for various solid tumors. *Mol Ther*. 2010;18:429-34.

Figure Legends

Fig. 1 Cytotoxic effect of KillerRed in association with intracellular reactive oxygen species and apoptosis in human cancer H1299 cells after light irradiation. **A**, parental H1299 cells and stable transfectants expressing KillerRed (H1299-KillerRed) or TurboFP635 (H1299-TurboFP635) were irradiated with green light for 60 min. Photobleaching and morphological changes were evaluated using fluorescent microscopy (IX71; Olympus). Scale bar: 100 μ m. **B**, H1299 and H1299-KillerRed cells were irradiated with or without green light for 10 min. To measure reactive oxygen species, irradiated and non-irradiated cells were incubated with DCF-DA solution (20 μ M) for 30 min at 37 °C and were then washed twice with PBS. Fluorescence intensity was measured at 485/528 nm using a fluorescence microplate reader. DCF fluorescence data are expressed as mean values \pm SD (n = 5). Statistical significance was determined using Student's *t* test. *, *P* < 0.05. **C**, immunocytochemical analysis of apoptosis in H1299-KillerRed cells after light irradiation. H1299-KillerRed cells were irradiated with green light for 60 min. Twenty-four hours after irradiation, the H1299-KillerRed cells were fixed with 3% paraformaldehyde solution for 15 min and were then incubated with rabbit anti-cleaved caspase-3 monoclonal antibody and FITC-conjugated secondary antibody. After nuclear staining with DAPI, the cells were observed under a fluorescent microscope (IX71; Olympus). Scale bar: 100 μ m.

Fig. 2 Photobleaching and morphological changes in human cancer cells infected with Ad-KillerRed or Ad-TurboFP635 after light irradiation. H1299, HCT116 and HT-29 cells were infected with replication-deficient adenovirus vectors expressing KillerRed

(Ad-KillerRed) or TurboFP635 (Ad-TurboFP635) at an MOI of 100 MOI for 48 hours. After infection, virus-infected cells were irradiated with green light for 60 min. Photobleaching and morphological changes were evaluated using fluorescent microscopy (IX71; Olympus). Scale bar: 100 μ m.

Fig. 3 Decreased viability of human cancer cells infected with Ad-KillerRed after light irradiation. **A**, Irradiation time-dependent photobleaching and decreased viability of H1299 cells infected with Ad-KillerRed at 100 MOI. Scale bar: 100 μ m. **B, C**, H1299, HCT116 and HT-29 cells were infected with Ad-KillerRed (**B**) or Ad-TurboFP635 (**C**) at the indicated MOIs for 48 hours and cell viability was measured using the XTT assay immediately after irradiation with or without green light for 60 min. Cell viability was calculated relative to that of the mock-infected group, which was set at 100 percent. Cell viability data are expressed as mean values \pm SD (n = 5). Statistical significance was determined using Student's *t* test. *, *P* < 0.05.

Fig. 4 Time-dependent KillerRed upregulation and laser irradiation-induced decreased cell viability in human cancer cells infected with TelomeKiller. **A**, expression of the KillerRed protein in H1299 cells infected with a replication-deficient Ad-KillerRed (Ad-KR) virus or a telomerase-specific conditionally replicating TelomeKiller (CRAAd-KR) virus at an MOI of 100 for 72 hours. Parental H1299 cells and KillerRed-expressing stable transfectants H1299-KillerRed (H1299-KR) were used as the negative and positive control, respectively. Cell lysates were subjected to western blot analysis with an anti-KillerRed antibody. β -actin was assayed as a loading control. **B**, H1299, HCT116 and HT-29 cells were infected with

TelomeKiller at an MOI of 100 for 48 hours. After infection, the virus-infected cells were irradiated with green light for 60 min. Photobleaching and morphological changes were evaluated using fluorescent microscope (IX71; Olympus). Scale bar: 200 μm . **C**, H1299, HCT116 and HT-29 cells were infected with TelomeKiller at the indicated MOIs for 48 hours and cell viability was measured using the XTT assay immediately after irradiation with or without green light for 60 min. Cell viability was calculated relative to that of the mock-infected group, which was set at 100 percent. Cell viability data are expressed as mean values \pm SD ($n = 5$). Statistical significance was determined using Student's *t* test. *, $P < 0.05$.

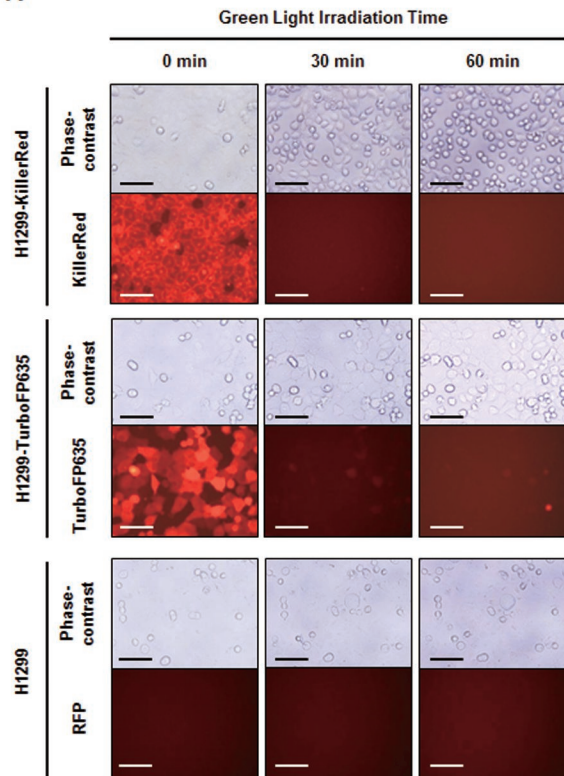
Fig. 5 Antitumor effect of TelomeKiller in subcutaneous HCT116 xenograft tumor model. **A**, Expression of red fluorescence in mice with bilateral HCT116 xenograft tumors injected with PBS (R, right tumor) or TelomeKiller (L, left tumor). **B**, Macroscopic appearance and distribution of red fluorescence in HCT116 tumors injected with PBS or TelomeKiller. Scale bar: 2 mm. **C**, Schedule of treatment and tumor growth curve of the subcutaneous HCT116 xenograft tumor model. Tumor growth is expressed as the mean tumor volume \pm SE ($n = 4$ or 5). Statistical significance was determined using Student's *t* test. *, $P < 0.05$. **D**, Macroscopic appearance of all isolated tumors in each group. **E**, Histopathological examination of excised tumors stained with hematoxylin and eosin. Left scale bar: 500 μm . Right scale bar: 100 μm . PDT, photodynamic therapy.

Fig. 6 TelomeKiller-mediated ablation of metastatic lymph nodes in combination with light irradiation. **A**, Macroscopic appearance of rectal tumor when virus was injected. Scale bar: 5

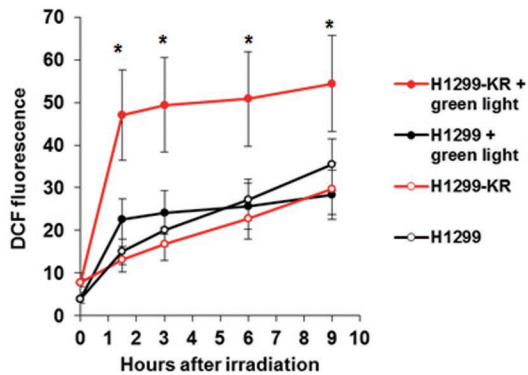
mm. **B**, Treatment and evaluation schedule for metastatic lymph nodes. **C**, Macroscopic and fluorescence images of the abdominal cavity at laparotomy. Scale bar: 1 mm. **D**, The GFP fluorescence intensity of metastatic lymph nodes in each group mouse was measured on days 0, 3 and 21. Data of each mouse are plotted individually.

Fig. 1

A



B



C

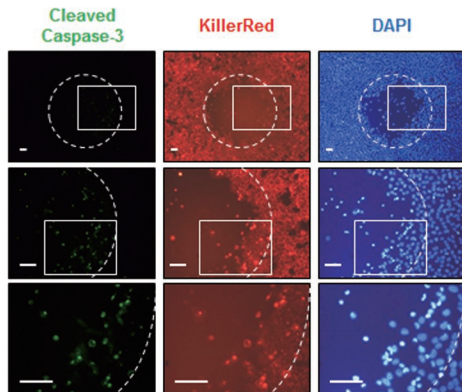


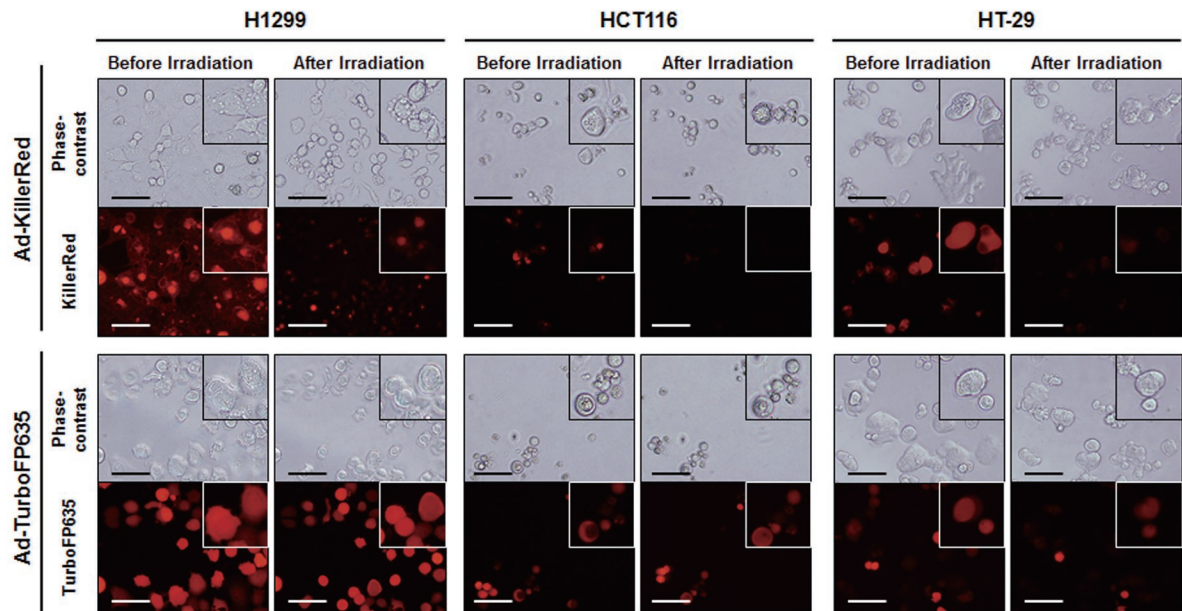
Fig. 2

Fig. 3

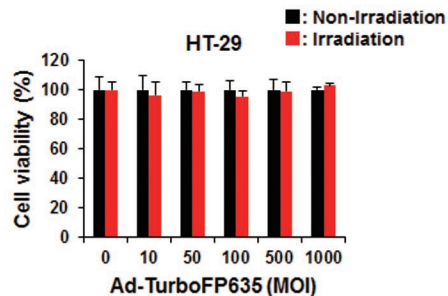
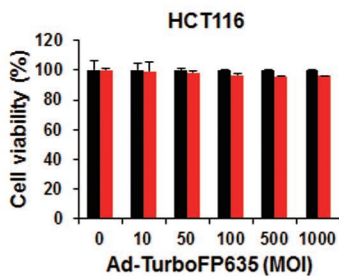
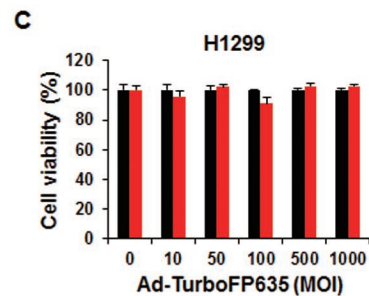
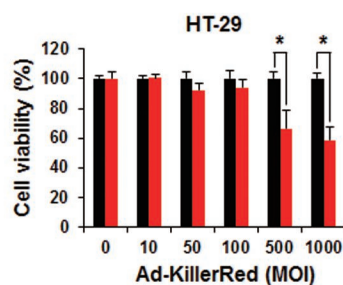
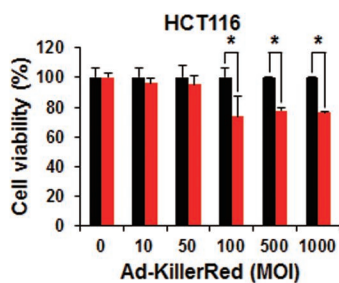
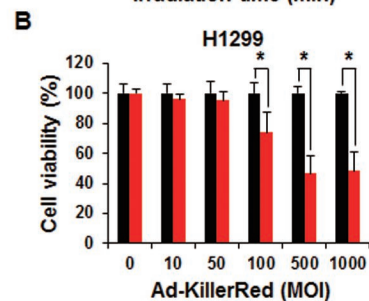
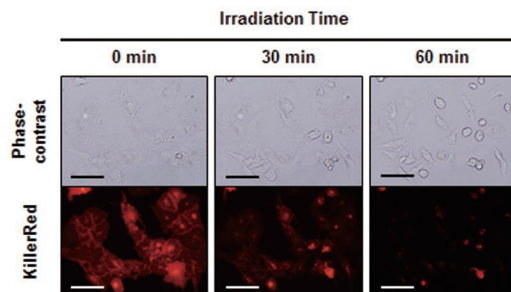
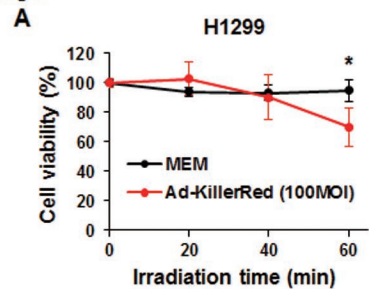
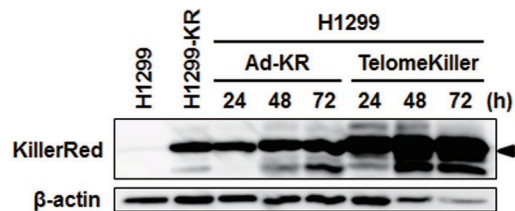
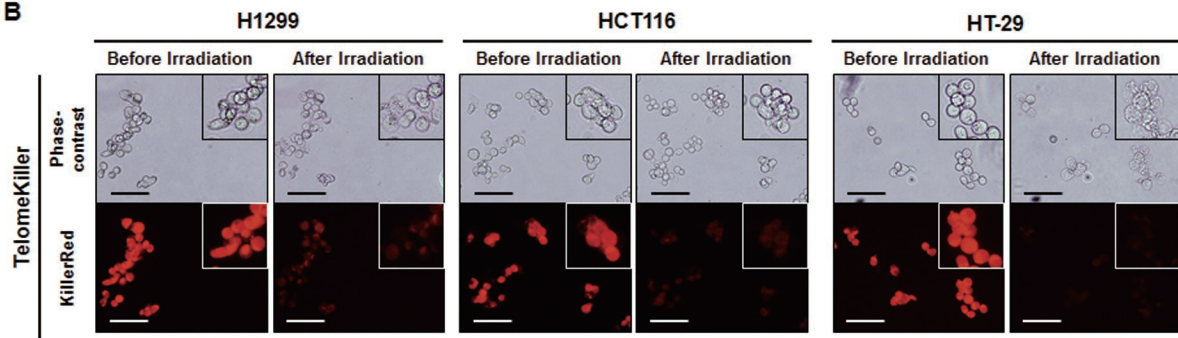


Fig. 4

A



B



C

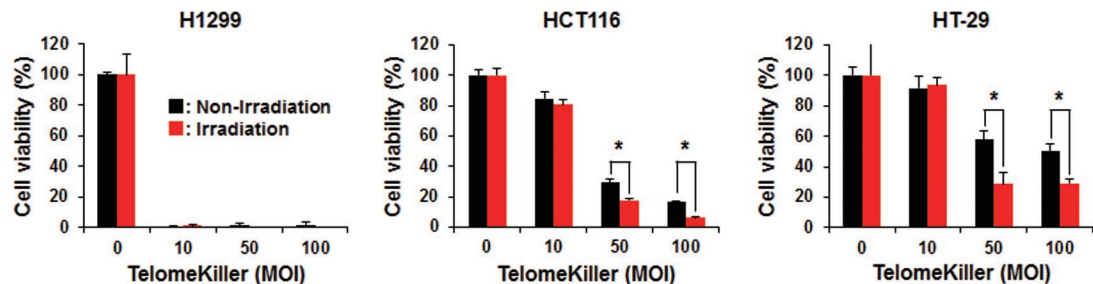
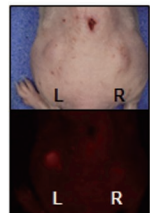
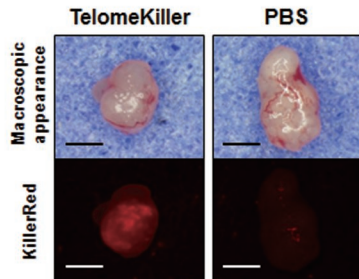


Fig. 5

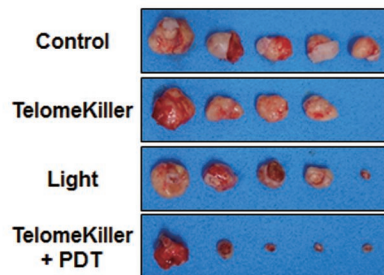
A

R: PBS
L: TelomeKiller

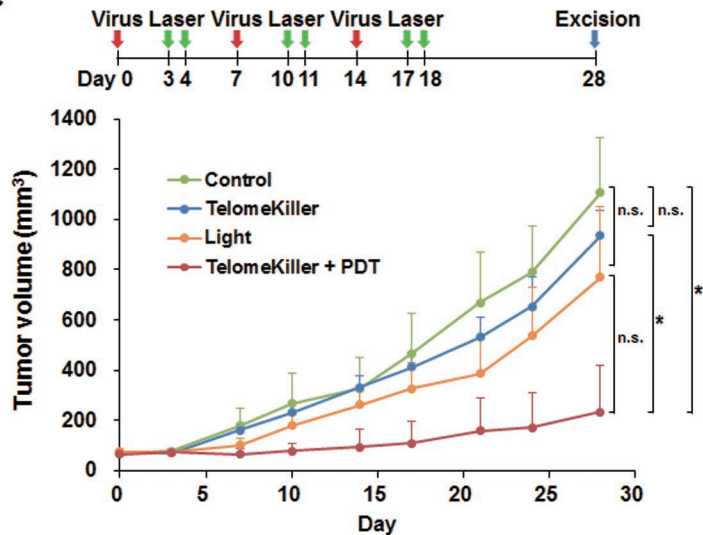
B



D



C



E

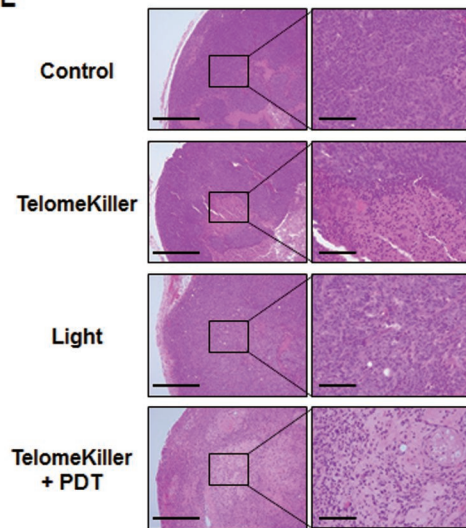
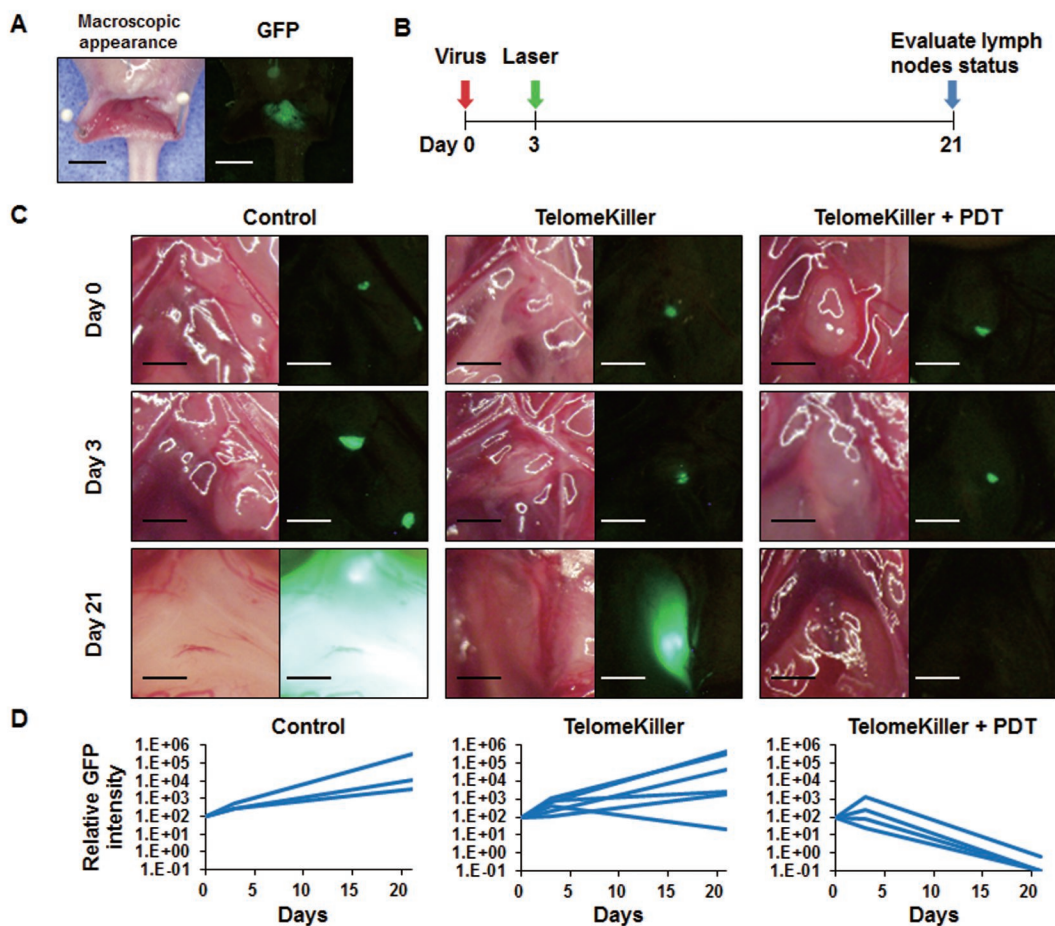


Fig. 6



Supplementary Data

**Takehara *et al.*
Targeted photodynamic virotherapy
armed with a genetically encoded photosensitizer**

Supplementary Fig. S1

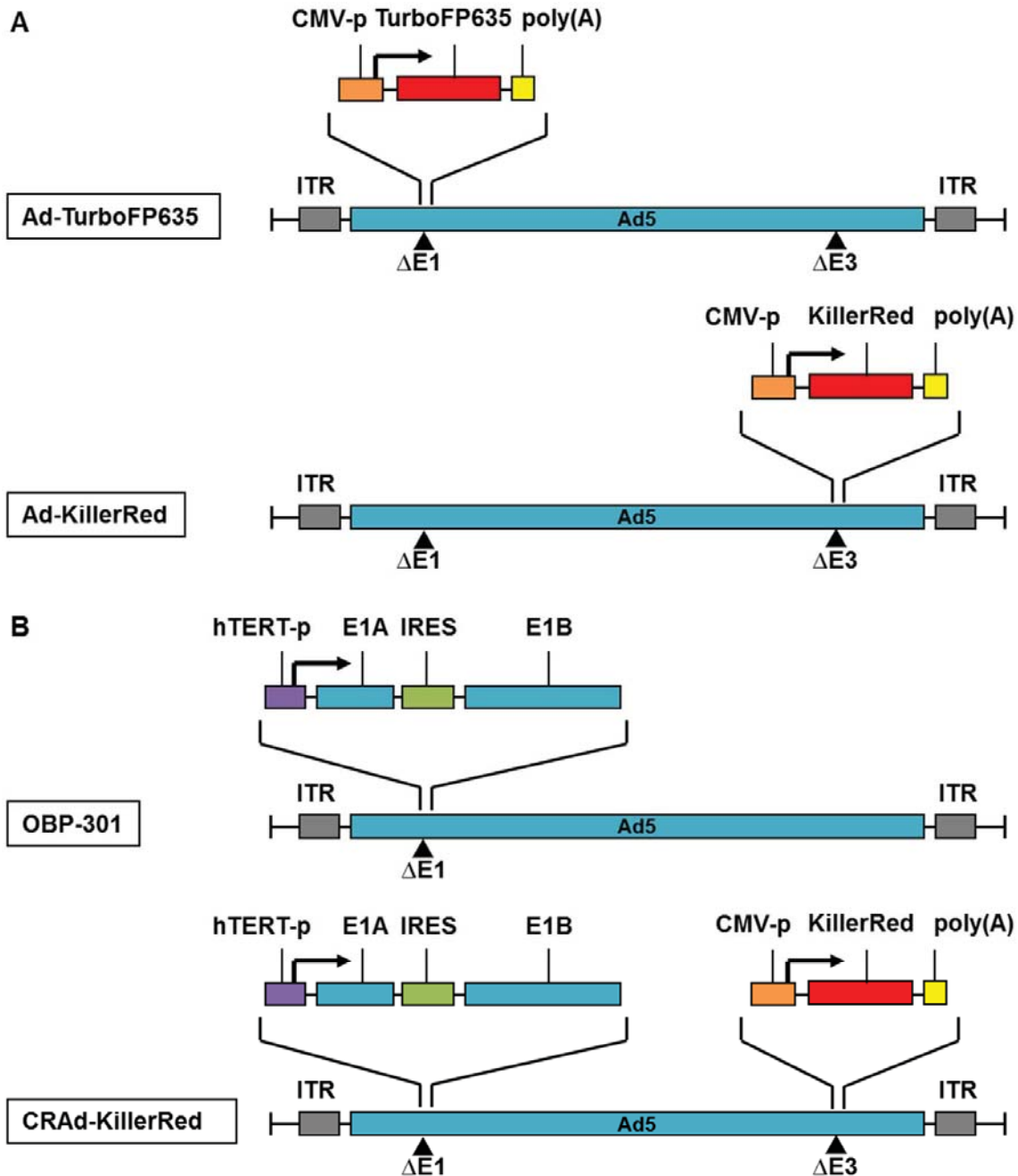
Schematic diagrams of the structures of replication-deficient and conditionally replicating adenovirus vectors.

Supplementary Fig. S2

The GFP fluorescence intensity of metastatic lymph nodes in HCT116-GFP-bearing mice after treatment with TelomeKiller and laser irradiation.

Supplementary Fig. S1

Schematic diagrams of the structures of replication-deficient and conditionally replicating adenovirus vectors.

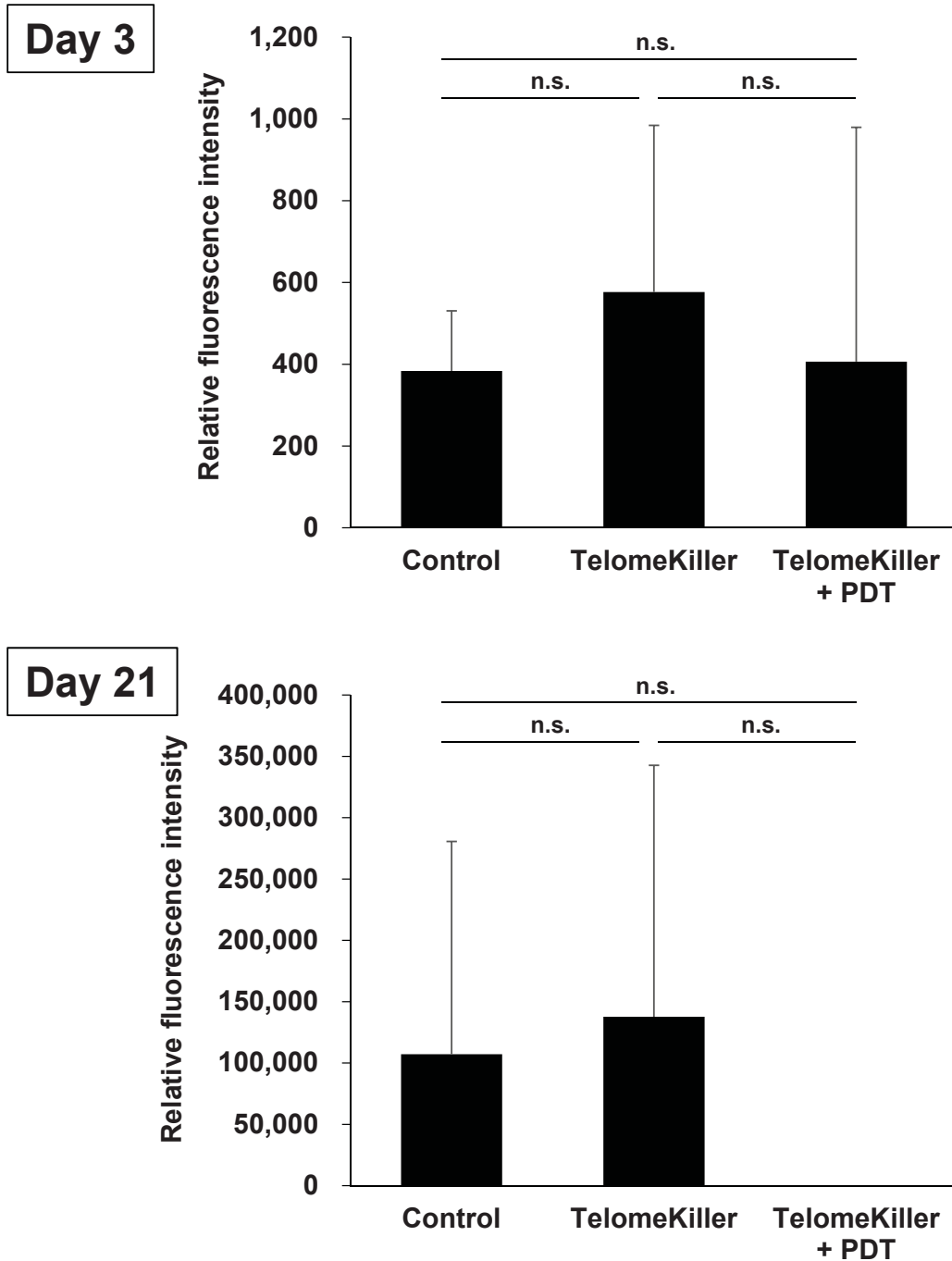


Supplementary Fig. S1

Schematic diagrams of the structures of replication-deficient and conditionally replicating adenovirus vectors. **A**, Ad-TurboFP635 and Ad-KillerRed are non-replicative E1/E3-deleted adenovirus vectors expressing TurboFP635 and KillerRed, respectively, under the regulation of the CMV promoter. **B**, OBP-301 is a telomerase-specific conditionally replicating adenovirus, in which the hTERT promoter drives the expression of E1A and E1B genes that are linked with an IRES. CRAAd-KillerRed is a KillerRed-armed OBP-301, in which the CMV promoter drives the expression of the KillerRed gene that is inserted into the E3 region.

Supplementary Fig. S2

The GFP fluorescence intensity of metastatic lymph nodes in HCT116-GFP-bearing mice after treatment with TelomeKiller and laser irradiation.



Supplementary Fig. S2

The GFP fluorescence intensity of metastatic lymph nodes in HCT116-GFP-bearing mice after treatment with TelomeKiller and laser irradiation. The values of GFP intensity at day 0 was set at 100, and relative mean GFP fluorescence intensity of metastatic lymph nodes was calculated in control, TelomeKiller, and TelomeKiller + PDT groups on days 3 and 21. n.s.; not significant.